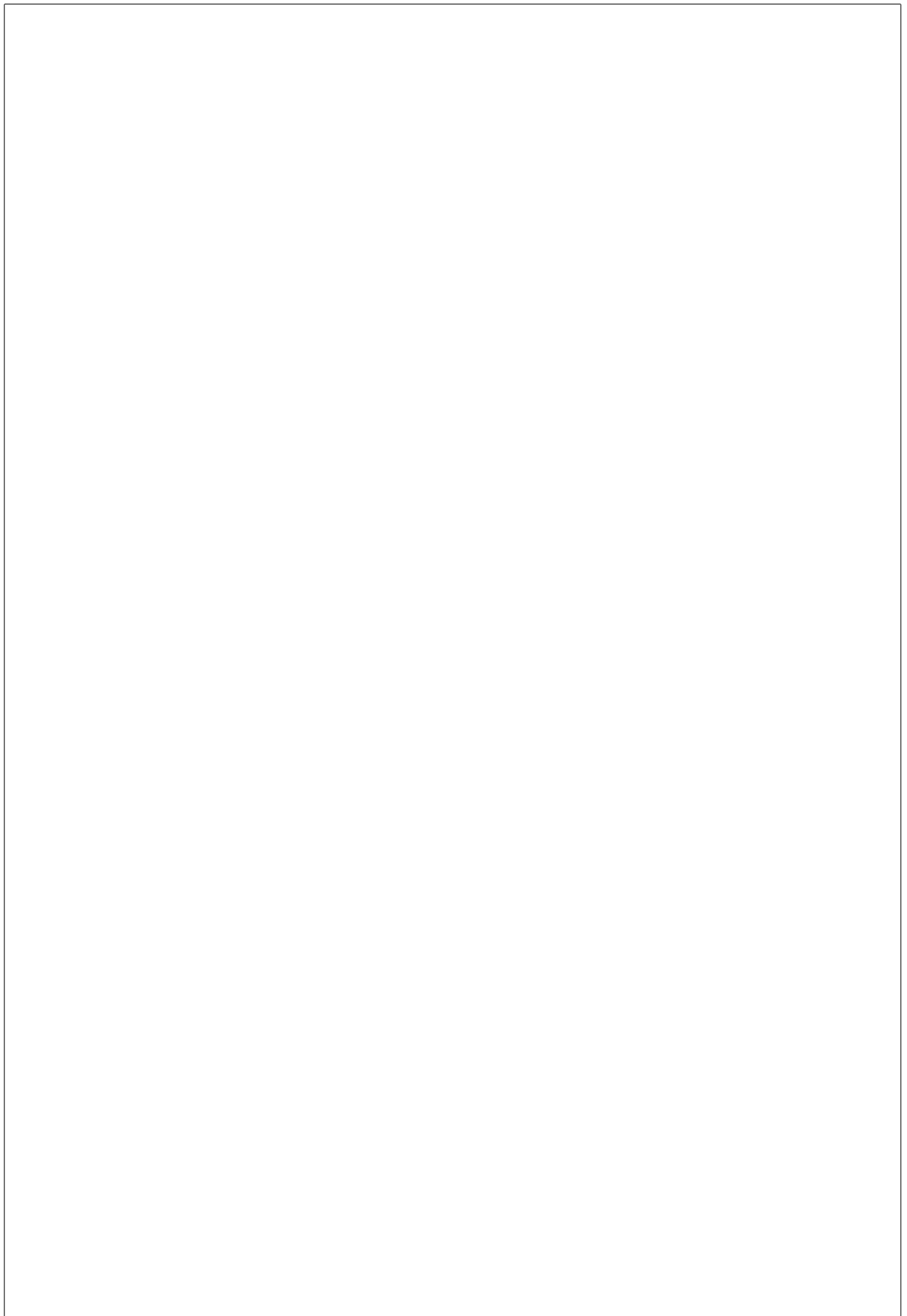


---

---



---

---

---

# Contents

<b>Table of Contents</b>	i
<b>List of Tables</b>	i
<b>1 Fabrication of Nanodiamonds</b>	1
1.1 HPHT . . . . .	2
1.2 CVD . . . . .	2
1.3 Wet-Milling . . . . .	5
1.3.1 Wet-Milled HPHT Nanodiamonds . . . . .	6
1.3.2 Wet-Milled CVD Nanodiamonds . . . . .	6
1.3.3 Doubly Wet-Milled Implanted Nanodiamonds Implanted With Silicon .	7
1.4 Iridium Substrate . . . . .	8
1.4.1 Preparation of The Substrate . . . . .	9
1.5 Listing of available samples . . . . .	10
<b>Summary and Conclusions</b>	12
<b>Bibliography</b>	13

---

---

# List of Tables

1.1	Samples grown with diamondoid seeds . . . . .	4
1.2	Listing of available wet-milled samples . . . . .	11

---

---

## Chapter 1

# Fabrication of Nanodiamonds

### Remark:

die section mit den silicon implanted nanodiamonds muss von dir ueberarbeitet werden. Die hab ich deshalb vorerst ausgelassen. Es gibt 3 teile (einfuehrung, preliminary tests und final procedure). Ich hab den eindruck, dass sich da konzeptionell vieles wiederholt und das man das ganze vielleicht in einer section unterbringen kann und die feineren unterscheidungen einfach beilaeufig erwaehnt.

“Diamond forms under high temperature and pressure conditions that exist only about 100 miles beneath the earth’s surface.”

Gemological Institute of America Inc.

Due to its extraordinary properties, diamond has transcended its sole purpose as a rare gem and developed into an important tool enabling various applications in industry and research. This change has been driven largely by the development of methods allowing to cheaply produce synthetic diamond. While synthetic diamonds are typically small and without the splendeur generally associated with diamond, they can be produced on-demand and are thus arguably more useful than rare gemstones. In this chapter we introduce the two most common methods for the fabrication of diamonds in a laboratory setting: The high-pressure, high-temperature and the chemical vapor deposition method. The aptly named high-pressure, high-temperature (HPHT) process mimics the conditions under which diamond is formed in nature and is widely used to synthetically produce diamonds for industrial applications such as utilization of diamond as a abrasive. While HPHT diamonds are utilized in this work, most reported measurements are based on diamond produced with the CVD method in which diamonds are grown using a hydrocarbon gas mixture. Both processes have incommon that defects and impurities are a naturally occurring. For a more extensive list of diamond production processes refer to [1]. In the context of this thesis nano-sized dimonds are required. They can be obtained by milling larger sized HPHT or CVD diamonds down to the desired grain size in a vibrational mill. The obtained nanodiamonds are small enough that individual specimen have a chance of hosting a singleton SiV center. These can be identified and used for further exploration.

## 1.1 High-Pressure High-Temperature Diamond

The HPHT method was the first process to successfully synthesize diamond in 1879. Today, it is still widely used due to its relatively cheap production costs for small diamonds [2]. In the HPHT process, diamond is synthesized from graphite under temperatures of up to  $1.5 \times 10^3$  °C pressures between  $5 \times 10^4$  bar and  $10^6$  bar [1]. Under these extreme conditions, carbon transitions from its graphite to its diamond phase because the latter becomes energetically favorable [?, ?, ?, ?]. The machine used for this kind of synthesis is a press. For some forms of this method, a metallic catalyst solvent is added lowering the required pressures and temperatures by causing graphite to dissolve earlier. At the same time the catalyst promotes the crystallisation process. Several press designs exist, all of which relying on creating and maintaining high pressures and a high temperatures. While it is possible to grow big ( $> 10$  carat) high-quality diamonds with the HPHT process, its cost quickly increases and thus becomes unfavorable.

In this thesis, HPHT nanodiamonds produced by Davydov et al. [3] are spectroscopically investigated.

## 1.2 Chemical Vapor Deposition Diamond

In contrast to the HPHT method, diamond is crystallized from carbon available in the gas phase in the CVD method. The process still requires respectable temperatures in the range of 700 °C to 1300 °C but makes due with the low pressures of less than 1 bar available in a vacuum growth chamber [?].

The chamber contains a vapour consisting of a mixture of atomic hydrogen and methane. The gas can be forced into the plasma phase using strong microwaves or hot filaments [?, ?, ?]. While the hot filament is easy to implement, it has the disadvantage that atoms which are etched from the filament during the growth process are likely to contaminate the diamond. To minimize the introduction of defects other than SiV centers in the diamond, growing diamonds in a microwave plasma is preferred. In it methane molecules dissociate and release carbon. In the presence of a substrate such as iridium containing suitable seeds, carbon can crystalize forming diamond. Figure 1.1 illustrates the setup. In a plasma containing atomic hydrogen, the formation of diamond is favored over the formation of graphite. This is due to the fact that the atomic hydrogen preferentially etches *sp*<sup>2</sup> bonded carbon, i.e. graphite.

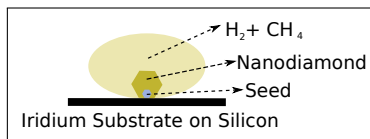


Figure 1.1: Sketch of the CVD method. A hydrogen-carbon plasma acts as a donor for carbon atoms which may crystallize to form diamond onto a suitable iridium substrate. An initial diamond seed facilitates the process.

Typically, single crystal diamond substrates are required to grow single crystal diamond. HPHT substrates are suitable to start a crystallization process. This approach is referred to as homoepitaxial growth. An alternative approach is to utilize non-diamond substrates such as iridium or platinum to trigger heteroepitaxial growth [?, ?]. This method is utilized for

all the CVD nanodiamonds grown and investigated in this thesis. It relies on small diamond crystals deposited in the substrate acting as seeds for the diamond crystallization process<sup>1</sup>. Seed diamond crystals are commercially available, and are usually particles produced by a so-called detonation process. In a detonation process, the high pressure produced by shock-waves of a detonation is used to create very small diamond particles of a size down to a few nanometers.

Growth on a substrate is favored, if the lattice constant of the substrate and the diamond to be grown are similar. The lattice constant of iridium is 0.384 nm [4, 5] and thus close to the lattice constant of diamond with 0.356 nm [6]. Therefore, the diamond was grown on a stratified substrate topped with an iridium layer of 60 nm to 150 nm thickness<sup>2</sup>. The iridium layers themselves were grown onto an yttria-stabilized zirconia (YSZ) buffer layer, which in turn was grown on a silicon wafer [7]. If the lattice constant of the substrate and the diamond are not matched, stress in the diamond lattice is induced. Therefore, the iridium substrate not only facilitates diamond growth, but also reduces unfavorable stress in the nanodiamonds. The detrimental effects of stress on the diamond lattice and its implications with respect to hosted SiV centers are briefly discussed in ??.

To produce nanodiamonds of controlled size, the growth process is stopped when the diamonds grown onto the seed crystals are large enough. If the growth process is continued, the individual crystals grow together to form diamond films. Such diamond films are used as starting material for the wet-milling process described in section 1.3.

One of the advantages of the CVD process is that silicon is incorporated automatically into diamonds, SiV centers can thus be formed *in-situ* as the diamond is grown. The presence of silicon atoms required to be absorbed into the diamond lattice is explained by the plasma etching the edges of the silicon waver underneath the growth substrate. To further increase the silicon content in the chamber, sacrificial silicon can be introduced.

After nanodiamond growth, the nanodiamonds are either investigated directly on the growth substrate or transferred to an ultrasonic bath to obtain a solution which is coated onto other substrates for further exorption.

In this thesis, two types of nanodiamond samples were investigated. The first batch, henceforth referred to as CVD samples, was grown by the group of M. Schreck, Augsburg University using detonation diamond seeds of a size smaller than 3 nm (produced by the company Microdiamant, product Liquid Diamond monocrystalline, MSY 0-0.03 micron GAF). For the growth process, 1 % of methane was added to the hydrogen environment in the growth chamber. The growth process was performed with a pressure of 30 hPa for 30 min to 60 min, yielding nanodiamonds of a diameter of about 100 nm to 200 nm. A sample of the produced diamonds is given in Figure 1.2.

The second type of samples consist of CVD nanodiamonds grown onto molecular analogs of diamond crystals. A subgroup of these molecular diamonds are called diamondoids and are carbon crystals based on the carbon cage molecule adamantane  $C_{10}H_{16}$ . The molecular diamonds used for this work are adamantane in cyclohexane, mercapto adamantane in cyclohexane, and cyclohexane. Each of these seed crystals was used in different growth processes. During the growth process, either 1 % or 3 % methane was added to the hydrogen plasma and either silicon (Si) or silicon dioxide ( $SiO_2$ ) was injected to promote the formation of *in-situ* incorporated SiV centers, see Table 1.1.

---

<sup>1</sup>CVD nanodiamond growth performed by S. Gsell, group of M. Schreck, Augsburg University

<sup>2</sup>Production of the stratified substrate performed by S. Gsell, group of M. Schreck, Augsburg University

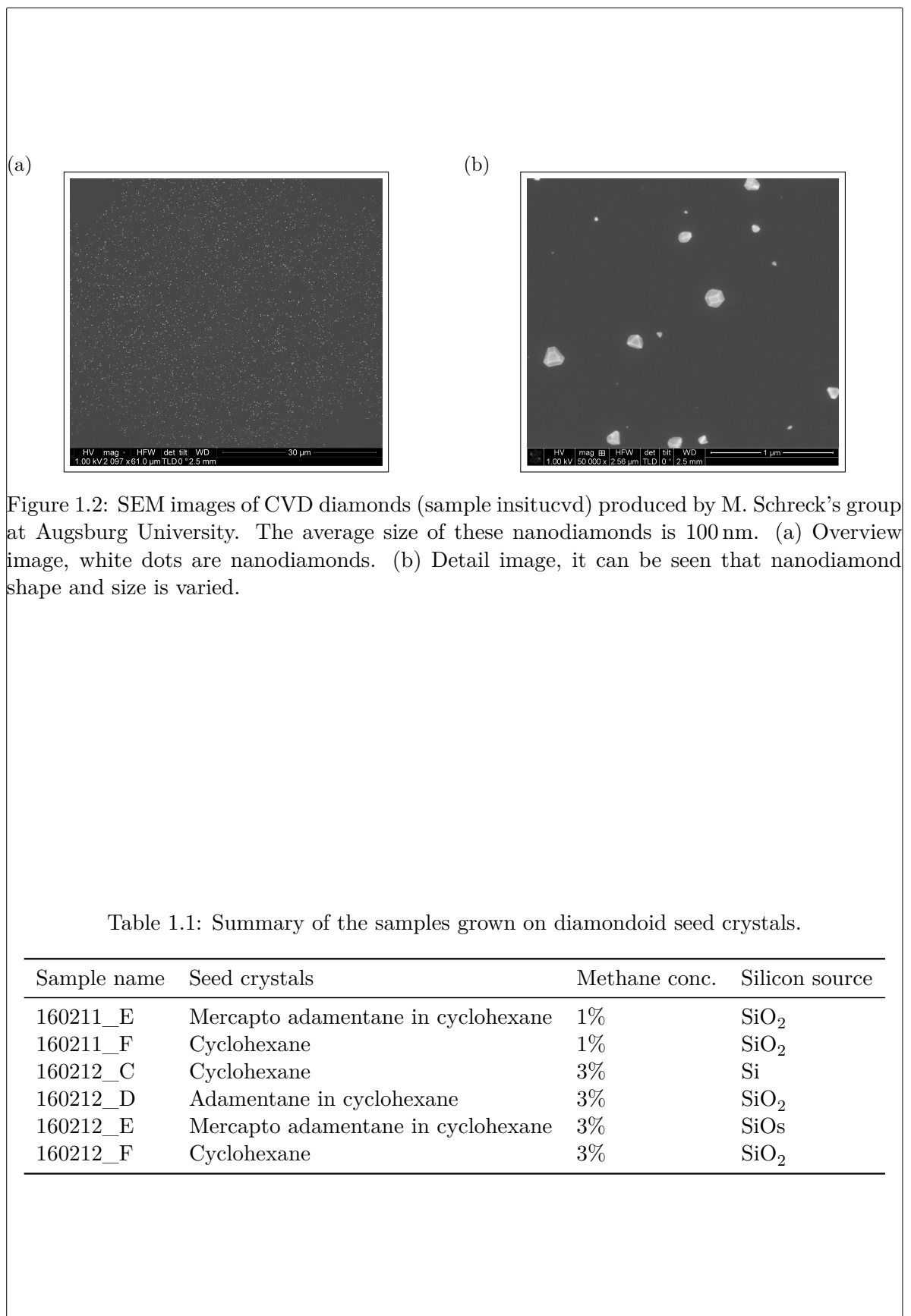


Figure 1.2: SEM images of CVD diamonds (sample insituvcvd) produced by M. Schreck's group at Augsburg University. The average size of these nanodiamonds is 100 nm. (a) Overview image, white dots are nanodiamonds. (b) Detail image, it can be seen that nanodiamond shape and size is varied.

Table 1.1: Summary of the samples grown on diamondoid seed crystals.

Sample name	Seed crystals	Methane conc.	Silicon source
160211_E	Mercapto adamentane in cyclohexane	1%	SiO <sub>2</sub>
160211_F	Cyclohexane	1%	SiO <sub>2</sub>
160212_C	Cyclohexane	3%	Si
160212_D	Adamentane in cyclohexane	3%	SiO <sub>2</sub>
160212_E	Mercapto adamentane in cyclohexane	3%	SiOs
160212_F	Cyclohexane	3%	SiO <sub>2</sub>

### 1.3 Wet-Milled Nanodiamonds

In addition to growing nanodiamonds of a specific size directly via a CVD process, macroscopic diamond starting material can be crushed to obtain small diamond particles. In contrast to nanodiamonds directly grown by a CVD process, the process is divided into two sub-processes: At first a macroscopic diamond is produced using one of the methods introduced in this chapter. Then macroscopic diamond is continuously milled into smaller diamond particles.

The wet-milled nanodiamonds investigated in this thesis were kindly provided by A. Muzha, group of A. Krueger, Julius-Maximilians Universität Würzburg. During the wet-milling process small metal beads in an aqueous solution are driven by the vibrations of a vibrational mill. The moving beads continuously collide with the present diamonds and thus keep breaking them into smaller and smaller particles. A sketch of the process is shown in ???. Steel contamination introduced by the beads can be eliminated in a post-processing treatment with acid.

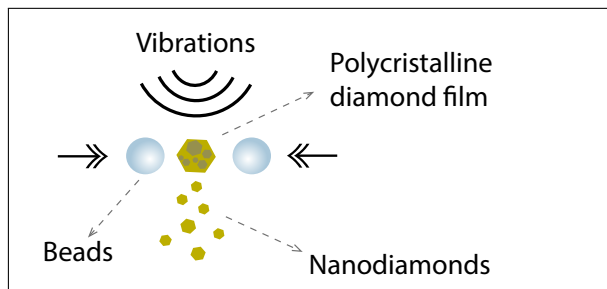


Figure 1.3: Sketch of a wet-milling process in a vibrational mill. A macroscopic polycrystalline nanodiamond is progressively broken down into smaller polycrystalline nanodiamonds by metal beads.

The big advantage of the milling process is that it enables the production of a large quantity of diamond nanoparticles. When producing nanodiamonds directly via a CVD process, the number of produced nanodiamonds in one process scales with the surface of the substrate on which the nanodiamonds are grown. In contrast, the quantity of milled nanodiamonds scales with the volume of the starting material. Another advantage of the wet-milling process is that the nanodiamonds are already in an aqueous solution after milling. Therefore, it can be used to spin-coat the nanodiamonds directly onto any substrate. Samples created in this fashion can directly be used for further investigation and do not require additional processing.

If the starting material for the wet-milling process is a polycrystalline diamond film, it is likely to break along distinct crystal boundaries. However, due to imperfections in the growth process, particles may break down such that progressively smaller milled diamond grain remain polycrystalline. As a result, the final nanodiamonds contain crystal boundaries themselves, indicative of reduced crystal quality. To improve diamond quality nanodiamonds are treated with post-processing steps including annealing in vacuum and oxidation in air. A detailed description of these processes and their effects is given in ??.

In general any diamond, independent of production method, can be used as starting material for the milling process. In the following sections, available samples are distinguished by the respective starting material and milling method.

### 1.3.1 Wet-Milled HPHT Nanodiamonds

We investigated nanodiamonds wet-milled from a HPHT starting material to median sizes of about 45 nm, 80 nm and 260 nm. They were then drop-cast onto an iridium substrate and implanted with  $^{28}\text{Si}^{1+}$ . The implantation itself was performed by D. Rogalla, Ruhr-Universität Bochum (RUBION - Zentrale Einrichtung für Ionenstrahlen und Radionuklide). All HPHT nanodiamonds were oxidized in air at 450 °C for 3 h. Resulting samples available for explorations are designated hphtimp45, hphtimp80, hphtimp260 and listed in Table 1.2.

Complete  
implanta-  
tion  
para-  
meters

### 1.3.2 Wet-Milled CVD Nanodiamonds

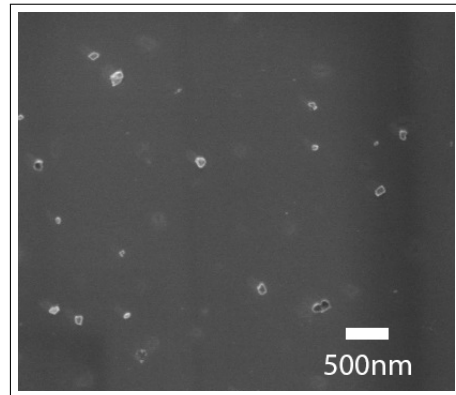


Figure 1.4: Pictures of milled nanodiamonds (sample insitu100) showing the distribution of the nanodiamond crystals on the iridium substrate.

In the following paragraphs, details of the production processes of nanodiamond produced by wet-milling a CVD diamond film in a vibrational mill are given. For an overview of the samples refer to Table 1.2. The starting material for the wet-milled nanodiamonds was a nanocrystalline diamond film [8] directly grown on a silicon wafer by CVD. A microwave hydrogen plasma containing 1% methane was used to grow on purified 5 nm nanodiamond seeds (produced by PlasmaChem). To induce *in-situ* SiV center creation, sacrificial Silicon pieces are placed in the growth chamber. During diamond growth the silicon pieces are etched by the plasma leading to individual atoms being incorporated into the diamond lattice. The diamond film is then wet-milled in a vibrational mill with steel beads. The high amount of steel containment due to the steel beads is removed by extensive acid treatment. We also investigated nanodiamonds milled with silicon nitride beads, and found that the choice of material of the beads does not result in any noticeable difference in dependent measurements. The median diameters of the diamonds are 50 nm, 70 nm and 100 nm as determined by laser diffraction spectroscopy. ?? shows milled nanodiamonds ontop of an iridium substrate. The aqueous solution containing the nanodiamonds is drop cast onto an iridium film on a Silicon substrate. The iridium film of a thickness of 130 nm is grown onto a buffer layer of yttria-stabilized zirconia (YSZ) which in turn is grown onto a Silicon wafer. The iridium surface has the advantage that it acts as an antenna and therefore enhances the collection efficiency of fluorescence light [9]. For a discussion on the properties of the substrate see section 1.4. Post-process treatment consist of annealing in vacuum at 900 °C or consecutive oxidation in air at a temperature of 450 °C, or a combination of the two. The duration for either treatment

method was 3 h to 6 h.

### 1.3.3 Doubly Wet-Milled Implanted Nanodiamonds Implanted With Silicon

In addition to SiV centers that were implanted during diamond growth, we investigated nanodiamonds with SiV centers implanted after diamond growth. Here a polycrystalline Element Six diamond film (electronic grade) served as the starting material. In bulk material, the implantation causes the SiV centers to form in a specific depth dependent on the implantation energy, leaving most of the diamond vacant of SiV centers. As a consequence, a big portion of nanodiamonds milled from such a bulk material would not host any SiV centers. To obtain diamond particles with a homogeneous distribution of SiV centers, the process of fabricating implanted nanodiamonds is the following: First, the diamond film is milled to diamond particles a few microns in size. Next, these microdiamonds are spin-coated onto iridium substrates and implanted with  $^{28}\text{Si}^{1+}$ . To eliminate lattice damage and unnecessary vacancies resulting from the implantation process, diamonds were annealed in vacuum and subsequently oxidized. At last, the micrometer sized diamond particles are milled to the desired smaller sizes.

#### Preliminary Tests

The starting material was an Element Six electronic grade diamond film. The diamond was milled in a wet-milling process to sizes on the order of micrometers, which were then coated onto a silicon substrate. The microdiamonds were implanted with  $^{28}\text{Si}^{1+}$  at an implantation energy of 1.7 MeV, and fluences of  $10^9 \text{ cm}^{-1}$  to  $10^{12} \text{ cm}^{-1}$ <sup>3</sup>. After implantation, the microdiamonds on the silicon substrate were annealed for 2 h at 900 °C and oxidized in air for another 2 h at 450 °C. However, we encountered the problem that the silicon sublimated and re-nucleated during annealing, causing the diamonds to sink into the silicon surface (Figure 1.5a). Iridium is less prone to damage by high temperatures and withstands annealing procedures up to our standard annealing temperature of 900 °C without problems. Therefore, we used a sample with microdiamonds on a silicon substrate which was not annealed to shake the nanodiamonds off the silicon substrate in an ultrasonic bath, and consecutively coated the microdiamonds on an iridium substrate. After annealing and oxidizing the nanodiamonds on the iridium substrate, the iridium surface was intact.

#### Final Procedure

For the milling process in a vibrational mill, a minimum amount of diamond material is necessary. When starting with a diamond film, this threshold is easily reached, however, a big quantity of microdiamonds is needed to meet the requirements. Therefore, production was carried out at a larger scale after the preliminary tests. The microdiamonds were directly spin-coated onto iridium substrates, implanted with  $^{28}\text{Si}^{1+}$  (implantation energy 900 keV, fluence  $10^{11} \text{ cm}^{-2}$ )<sup>4</sup>. The microdiamonds were then annealed in vacuum for 3 h at 900 °C and oxidized

how  
much?

<sup>3</sup>Implantation performed by D. Rogalla, Ruhr-Universität Bochum (RUBION - Zentrale Einrichtung für Ionenstrahlen und Radionuklide).

<sup>4</sup>Implantation performed by J. Klug at rubitec - Gesellschaft für Innovation und Technologie der Ruhr-Universität Bochum mbH.

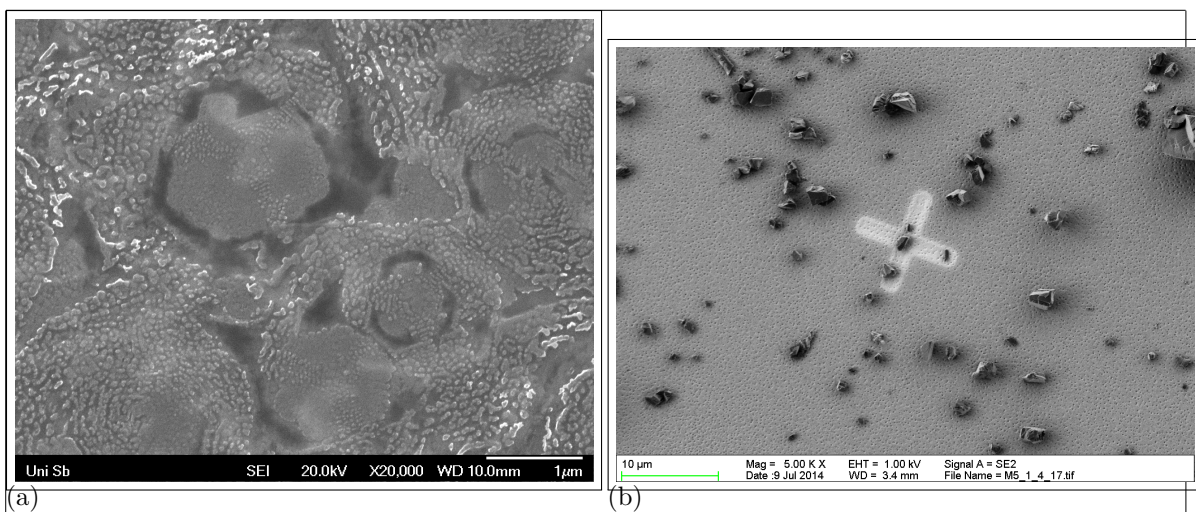


Figure 1.5: (a) SEM picture of nanodiamonds sunken into a silicon substrate after annealing at 900 °C for 3 h. Magnification 20 000. (b) SEM image of the microdiamonds after milling on an iridium substrate, but before implantation. In the middle of the picture, there is a reference cross milled into the iridium substrate with a focused ion beam. Its size amounts to 10  $\mu\text{m}$ . It can be seen, that the microdiamonds exhibit sizes of a few micrometer.

in air for 3 h at 450 °C. At last, they were milled again to sizes of about 40 nm, 45 nm, 240 nm and 260 nm. The diamonds of sizes 40 nm and 240 nm were annealed in vacuum at 1200 °C.

time?

## 1.4 Iridium Substrate

As mentioned in section 1.2, growth on a substrate is favored, if the lattice constant of the substrate and the diamond to be grown are similar. Therefore, for CVD nanodiamond growth a multilayered substrate was prepared in a heteroepitaxial growth process. This substrate consists of a silicon wafer on the bottom, a yttria-stabilized zirconia buffer layer in the middle and an iridium layer on top. Initially, whole 4 in wafers were prepared with a multilayered structure. After the heteroepitaxial growth processes, the wafer is cut to squares with a side length of 1 cm to fit into all machinery used during experiments, such as the spin-coater, the confocal setup, the focussed ion beam and the SEM.

Apart from the favorable lattice constant, iridium exhibits further advantages which lead us to coating the wet-milled diamonds onto these same multilayered substrates:

- The high hydrophilicity of iridium enhances the homogeneity of the nanodiamonds on the substrate after spin-coating or drop-casting. The hydrophilicity is further improved by treating the substrate in a Piranha etch (50:50 mixture of sulfuric acid H<sub>2</sub>SO<sub>4</sub> and hydrogen peroxide H<sub>2</sub>O<sub>2</sub>) by removing oxide layers on the surface. The treatment with Piranha etch also has the advantage that all organic contamination is removed. Measurements after applying the Piranha cleaning yielded an estimation of the contact angle of slightly more than one degree. To determine the contact angle with water, the volume of a water drop is compared to the surface it covers after dropping it onto an iridium substrate, see Figure 1.6a. From that an estimation of the contact angle is deduced.

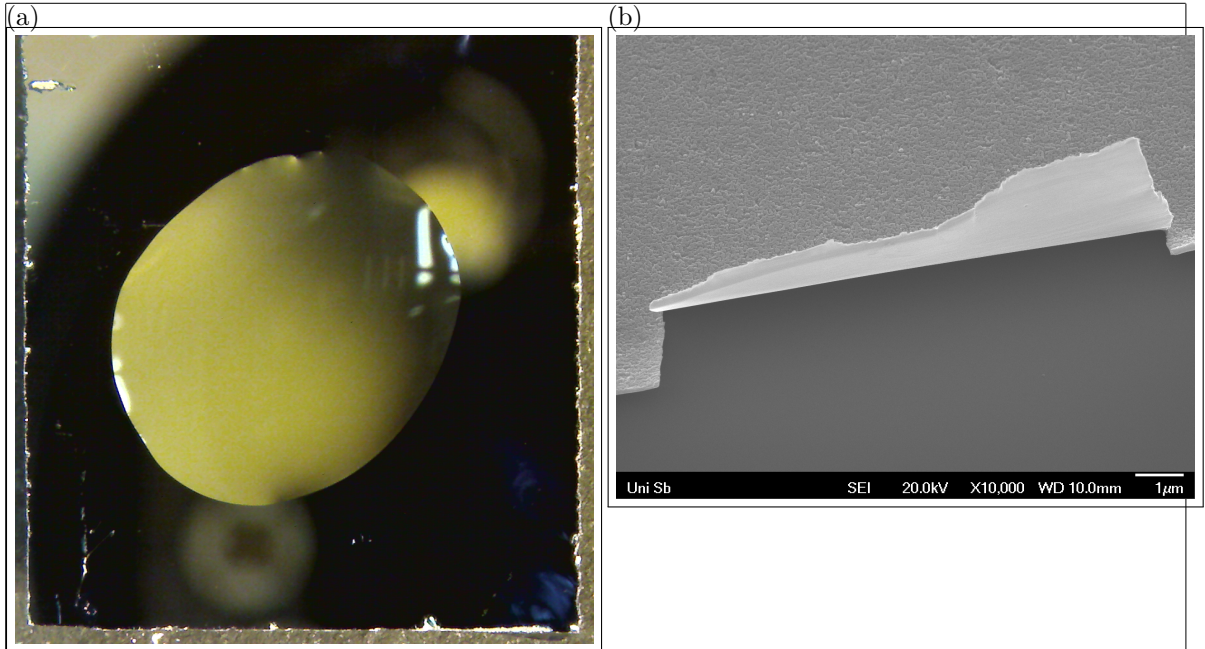


Figure 1.6: (a) Microscope image of a drop of water on an iridium substrate cleaned with Piranha etch. This picture was used to estimate the contact angle. (b) SEM picture of a 60 nm iridium layer that peeled off the substrate after an ultrasonic bath.

- During the post-processing steps, it is of major importance, that the substrate can withstand high temperatures. As described in section 1.3.3, during the preliminary tests with implanted nanodiamonds on a silicon substrate we encountered difficulties with diamonds on a silicon substrate as they sunk into the surface after annealing. In contrast, iridium withstands the high temperatures required for annealing without damage.
- Iridium acts both as a mirror and as an antenna for the fluorescence light emitted by the SiV center [9]. Therefore, the collection efficiency of the fluorescence light is enhanced.

At this point we comment upon a minor complication we experienced when using iridium surfaces. If the iridium layer is too thin, it tends to peel off the substrate, see Figure 1.6b. We encountered this problem during a cleaning procedure in the ultrasonic bath. However, this disadvantage is easily circumvented by using a thicker iridium layer. For our measurements, we used an iridium layer of a thickness of 130 nm, for which we did not encounter any adhesion problems.

#### 1.4.1 Preparation of The Substrate

Prior to drop-casting or spin-coating a diamond solution onto the iridium substrate, the substrate is cleaned. The standard cleaning procedure is started with treating the substrate in diverse chemicals in an ultrasonic bath. Each step is carried out for a duration of 3 min to 7 min, approximately adjusted to the amount of contamination present:

- Distilled water with a drop of dishwasher detergent: removes coarse contamination off

the substrate.

- Isopropanol (purity 99.9 % p.a.): dissolves oils without leaving oil traces as compared to ethanol
- Acetone (purity 99.9 % p.a.): a heavy-duty degreaser, also dissolves many plastics
- Distilled water: Acetone heavily reacts with the later applied Piranha solution, potentially causing explosions. Therefore, any acetone residue has to be removed. As acetone is water-soluble, distilled water is used to remove the residue.

Thereafter, the substrates are put into a Piranha solution (50 % sulfuric acid  $H_2SO_4$ , 50 % hydrogen peroxide  $H_2O_2$ ) to enhance the surface hydrophilicity and therefore obtain a homogeneous distribution of diamonds on the surface. They are then put again into distilled water and blow-dried with compressed air to avoid residue from the water.

The substrates were then either drop-casted or spin-coated with aqueous diamond solutions. For the former, the substrates are heated on a heating plate to a temperature of 60 °C. While the substrates are permanently heated by the heating plate, drops of a volume of about 5 µL are dropped onto the substrate surface. If substantially more than 5 µL is needed, then several drops of about 5 µL are dropped onto the substrate consecutively. A single large drop is ill-advised since the solution would flow off the substrate before drying.

For spin-coating, an on-site built spin coater was used. Therefore the spin-coater is pre-set to velocity of 2500 rpm. Then drops of 5 µL are dropped on the substrate and the spin-coater is immediately turned on. After about 3 min, the drop has dried. If more than 5 µL of diamond solution is wanted, the spin-coating is repeated until the desired amount is reached.

## 1.5 Listing of available samples

Table 1.2: Listing of available wet-milled samples. The first column indicates the names of the samples, the second the mean diameter of the nanodiamonds, and the third designates how the silicon was incorporated into the diamond.

Sample name	Size	Si incorporation	Post-processing
hphtimp45	45 nm	<i>implanted</i>	oxidized in air at 450 °C
hphtimp80	80 nm	<i>in-situ</i>	annealed in vacuum for 1 h at 1000 °C and at 900 °C for 3 h
hphtimp260	260 nm	<i>in-situ</i>	oxidized in air at 450 °C
insitu50	50 nm	<i>in-situ</i>	series of individual samples with diverse post-processing steps
insitu70	70 nm	<i>in-situ</i>	series of individual samples with diverse post-processing steps
insitu70n	70 nm	<i>in-situ</i>	no post-processing subset of insitu70
insitu70o	70 nm	<i>in-situ</i>	oxidized in air at 450 °C subset of insitu70
insitu100	100 nm	<i>in-situ</i>	series of individual samples with diverse post-processing steps
insitu100ao	100 nm	<i>in-situ</i>	annealed in vacuum at 900 °C, consecutively oxidized in air at 450 °C subset of insitu100
implanted250ao	250 nm	implanted	annealed in vacuum at 900 °C, consecutively oxidized in air at 450 °C
hphtimp260	40 nm	implanted	annealed in vacuum at 1200 °C, consecutively oxidized in air at 450 °C
hphtimp260	50 nm	implanted	oxidized in air at 450 °C
hphtimp260	240 nm	implanted	annealed in vacuum at 1200 °C, consecutively oxidized in air at 450 °C
hphtimp260	260 nm	implanted	oxidized in air at 450 °C

---

---

## Summary and Conclusions

In conclusion we found a strongly inhomogeneous distribution of SiV center spectra in nanodiamonds. We group the zero-phonon-lines into two groups: Group H consists of ZPLs exhibiting a narrow linewidth from below 1 nm up to 4 nm and a broad distribution of center wavelength between 710 nm and 840 nm. Compared to that, group V comprises ZPLs with a broad linewidth between just below 5 nm and 17 nm and center wavelength ranging from 730 nm to 742 nm. This data is consistent with previously measured SiV spectra [10, 11]. For comparison, an SiV center in unstrained bulk diamond exhibits a linewidth of 4 nm to 5 nm at a center wavelength of 737.2 nm [12, 13]. We show that both the observed blue-shift and the observed red-shift of group V are consistently explained by strain in the diamond lattice. Further, we suggest, that group H might be comprised of modified SiV centers, the structure of which is currently unclear.

We investigated the SiV sidebands: In group V we found one prominent peak at a shift of 42 meV, which corresponds to a well-known feature assigned to non-localized lattice vibrations [14, 15]. In group H we see an accumulation of peaks, at around 43 meV, 64 meV, 150 meV and 175 meV, which are consistent with sideband peaks reported in [15, 16, 17].

We further reported photon autocorrelation measurements which verified the existence of single SiV centers both in group H and group V. Investigating the time trace of the SiV center photoluminescence, we found that some SiV centers exhibit fluorescence intermittence with on times between several microseconds up to 41 s. Furthermore, we see an exponential distribution of bright time intervals and a log-normal distribution of dark time intervals, consistent with research on single molecules [18]. In terms of photostability, there is a big difference between group V and group H: All but one emitters in group H exhibit blinking, where only one of the emitters in group V exhibits blinking.

adding momentum towards the adoption of the quantum candela ...

# Bibliography

- [1] R F Davis. *Diamond Films and Coatings: Development, Properties, and Applications*. H{é}bert, Alexandre-Martin-Stanislas. Noyes Pub., 1993. 1, 2
  - [2] K H O'Donovan. Synthetic diamond. 2
  - [3] Valery a. Davydov, a. V. Rakhmanina, S. G. Lyapin, I. D. Illichev, K. N. Boldyrev, a. a. Shiryaev, and Viatcheslav N. Agafonov. Production of nano- and microdiamonds with Si-V and N-V luminescent centers at high pressures in systems based on mixtures of hydrocarbon and fluorocarbon compounds. *JETP Letters*, 99(10):585–589, 2014. 2
  - [4] John W. Arblaster. Crystallographic Properties of Iridium. *Platinum Metals Review*, 54(2):93–102, 2010. 3
  - [5] S. Gsell, M. Fischer, R. Brescia, M. Schreck, P. Huber, F. Bayer, B. Stritzker, and D. G. Schlom. Reduction of mosaic spread using iridium interlayers: A route to improved oxide heteroepitaxy on silicon. *Applied Physics Letters*, 91(6):061501, aug 2007. 3
  - [6] Robert F. Davis, editor. *Diamond Films and Coatings*. Noyes Pub., 1993. 3
  - [7] S. Gsell, T. Bauer, J. Goldfuß, M. Schreck, and B. Stritzker. A route to diamond wafers by epitaxial deposition on silicon via iridium/yttria-stabilized zirconia buffer layers. *Applied Physics Letters*, 84(22):4541, may 2004. 3
  - [8] Oliver A. Williams and Milos Č Nesládek. Growth and properties of nanocrystalline diamond films. *Phys. status solidi*, 203(13):3375–3386, oct 2006. 6
  - [9] Elke Neu, Mario Agio, and Christoph Becher. Photophysics of single silicon vacancy centers in diamond: implications for single photon emission. *Optics Express*, 20:19956–19971, jul 2012. 6, 9
  - [10] Julia Benedikter, Hanno Kaupp, Thomas Hümmer, Yuejiang Liang, Alexander Bommer, Christoph Becher, Anke Krueger, Jason M. Smith, Theodor W. Hänsch, and David Hunger. Cavity-Enhanced Single-Photon Source Based on the Silicon-Vacancy Center in Diamond. *Physical Review Applied*, 7(2):024031, 2017. 12
  - [11] Elke Katja Neu. *Silicon vacancy color centers in chemical vapor deposition diamond : new insights into promising solid state single photon sources*. PhD thesis, 2012. 12
  - [12] Carsten Arend, Jonas Nils Becker, Hadwig Sternschulte, Doris Steinmüller-Nethl, and Christoph Becher. Photoluminescence excitation and spectral hole burning spectroscopy of silicon vacancy centers in diamond. *Physical Review B*, 94(4):045203, jul 2016. 12

- [13] Andreas Dietrich, Kay D Jahnke, Jan M Binder, Tokuyuki Teraji, Junichi Isoya, Lachlan J Rogers, and Fedor Jelezko. Isotopically varying spectral features of silicon-vacancy in diamond. *New J. Phys.*, 16(11):113019, nov 2014. 12
- [14] F P Larkins and A M Stoneham. Lattice distortion near vacancies in diamond and silicon. I. *Journal of Physics C: Solid State Physics*, 4(2):143–153, feb 1971. 12
- [15] H. Sternschulte, K. Thonke, R. Sauer, P. C. Münzinger, and P. Michler. 1.681-eV luminescence center in chemical-vapor-deposited homoepitaxial diamond films. *Physical Review B*, 50(19):14554–14560, nov 1994. 12
- [16] AM Zaitsev. *Optical properties of diamond: a data handbook*. 2001. 12
- [17] Elke Neu, Martin Fischer, Stefan Gsell, Matthias Schreck, and Christoph Becher. Fluorescence and polarization spectroscopy of single silicon vacancy centers in heteroepitaxial nanodiamonds on iridium. *Phys. Rev. B*, 84(20):205211, nov 2011. 12
- [18] Natalie Z. Wong, Alana F. Ogata, and Kristin L. Wustholz. Dispersive Electron-Transfer Kinetics from Single Molecules on TiO<sub>2</sub> Nanoparticle Films. *The Journal of Physical Chemistry C*, 117(41):21075–21085, 2013. 12